29th Congress of the International Council of the Aeronautical Sciences
St. Petersburg, Russia; September 7-12, 2014

AERODYNAMIC DESIGN METHOD FOR SUPERSONIC SLENDER BODY USING AN INVERSE PROBLEM

Kisa Matsushima*, Ikki Yamamichi, Naoko Tokugawa*****
*** Dept. Engineering, University of Toyama, Gofuku 3190, Toyama 930-8555, JAPAN.**
Phone: +81-76-445-6796, Fax: +81-76-445-6796, Email: kisam@eng.u-toyama.ac.jp
**** Graduate Student, University of Toyama.**
***** Supersonic Aircraft Section, Japan Aerospace Exploration Agency.**

Keywords: *Supersonic slender bodies, Aerodynamic design, Inverse problems*

Abstract

Aiming to design the shape of SST fuselages of good aerodynamic performance, an efficient design system using personal level computers has been developed. This consists of CFD solvers and an inverse problem for shape design. The design system works well on SST nose of axisymmetric fuselage design as well as non-axisymmetric case.

1 Introduction

In supersonic flight, high fuel-efficiency and the reduction of sonic boom at cruising are crucial issues. Both phenomena are primarily connected with the pressure distributions on airplanes. In these two decades, a lot of work has been done for supersonic wing design to attain good aerodynamic performance [1, 2]. On the other hand, the design of fuselage is not well studied. In this article, considering important effects of pressure distribution on supersonic fuselage performance, an inverse problem is formulated and utilizing the inverse problem, a simple and efficient aerodynamic design system for supersonic fuselage shape is developed. The design system works well on SST nose design problems. The turn-around time to complete a design is short.

In Section 2, the formulation of an inverse problem is discussed. In Section 3, a design system is constructed to utilize the formulated inverse problem. To examine the ability of the design system, the design problems are solved in Sections 4 and 5. Section 4.

2 Formulation of an Inverse Problem for Slender Bodies of revolution in Supersonic Flows

2.1 The Perturbation Potential Equation in Cylindrical Coordinates

The formulation starts with a body of revolution located on a supersonic flow field which might follow the axially symmetric potential equation of Eq. (1) in cylindrical coordinates (*x, r, θ*).

$$(1 - M_\infty^2)\frac{\partial^2 \varphi}{\partial x^2} + \frac{\partial^2 \varphi}{\partial r^2} + \frac{1}{r}\frac{\partial \varphi}{\partial r} = 0 \qquad (1)$$

In Eq.(1), φ is the perturbation potential for perturbation velocity *u, v, w*, where M_∞ denotes the uniform flow Mach number. Its velocity speed is *U*. As for perturbed velocities, *u, v, w* correspond to *x, r, θ* coordinates, respectively. Here, the axial velocity *w* is 0, because we are thinking axially symmetric flow fields.

For the supersonic flows, introducing the notation, $\beta = \sqrt{M_\infty^2 - 1} > 0$, Eq.(1) could be solved to be the integral equation form[3];

$$\varphi(x,r) = -\int_0^{x-\beta r} \frac{f(\xi)}{\sqrt{(x-\xi)^2 - \beta^2 r^2}} d\xi \qquad (2)$$

where, ξ is a integral variable along the *x*-axis. In Eq.(2), $f(\xi)$ is unknown and should be determined by using a boundary condition, Eq.

(3). When the axisymmetric body surface contour is given by $r = R(x)$, the slip conditions there are described as

$$\frac{dR}{dx} = \frac{v_s}{U + u_s} \qquad (3)$$

where subscript s indicates physical quantity at the body surface. As readers know $v = \frac{\partial \varphi}{\partial r} =$ Function of $f(x)$, Eq.(3) relates $f(x)$ to velocity components. It also relates the fuselage geometry and velocity.

2.2 Pressure as a Function of Velocity

Let us define the relation between pressure distributions and velocity. First, we consider isentropic relation between pressure and velocity. Then, normalizing pressure by the free stream dynamic pressure and applying the first-order small perturbation theory, it yields the pressure coefficient.

$$Cp = -\frac{2u}{U} - \left(\frac{v}{U}\right)^2 \qquad (4)$$

2.3 Slender Body Approximation

For the supersonic flows about a slender body, Eq.(2) is to be transformed into the following form [1].

$$\varphi(x,r) = -f(x)\log\frac{2}{\beta\, r} - \int_0^x f'(\xi)\log(x-\xi)d\xi \quad (5)$$

Using Eq.(5), the radial velocity component is

$$v = \frac{\partial \varphi}{\partial r} = \frac{f(x)}{r} \qquad (6)$$

On the body surface, Eq.(6) is expressed

$$v_s = \frac{f(x)}{R} \quad \therefore f(x) = v_s R(x) \qquad (7)$$

Multiplying $R(x)$ and Eq.(3) and using Eq. (7), we obtain the concrete form of f.

$$R\frac{dR}{dx} = \frac{v_s R(x)}{U + u_s} = \frac{f(x)}{U + u_s}$$

or

$$\frac{d}{dx}\{R^2(x)\} = \frac{f(x)}{U + u_s} \qquad (8)$$

Furthermore, the polynomial expansion of u_s is applied to Eq(8) and take the first order approximation. Then, the area distribution function $S(x)$ of cross-flow sectional plane along the x axis is introduced. Finally, the equation of pressure coefficients yields the function of geometrical parameter that might be primitive equation of an inverse problem.

$$Cp = -\left(\frac{dR}{dx}\right)^2 + \frac{1}{\pi}S''(x)\log\frac{2}{\beta\, R} + \frac{1}{\pi}\frac{d}{dx}\int_0^x S''(\xi)\log(x-\xi)d\xi \qquad (9)$$

2.4 Solution for Slender Cone

Eqs. (8) and (9) is applied to the flow field about a slender cone whose nose angle is 2δ. In this case,

$$R(x) = x\tan\delta \approx x\delta + \frac{x}{3}\delta^3 \approx x\delta \qquad (10)$$

$$S(x) = \pi R^2 \approx \pi x^2 \delta^2 \qquad (11)$$

$$f(x) = xU\delta^2 \qquad (12)$$

Therefore, an equation to relate the pressure coefficient (Cp) and the nose angle parameter δ is formulated. It is one of essential equations in this article.

$$Cp = 2\delta^2 \log\frac{2}{\beta\delta} - \delta^2 \qquad (13)$$

2.5 Inverse Problem for Slender Cone

This section discusses the differential form of Eq.(13). The differential form is needed for the iterative residual correction design method that is explained later in Chapter 3. The idea is based on Taylor series expansion of Eq.(13) in terms of $\Delta\delta$, difference in δ. Neglecting second and higher order terms, we obtain simple mathematical model of Eq.(14).

$$\Delta Cp = g'(\delta)\Delta\delta \tag{14}$$

where $g(\delta) = 2\delta^2 \log\dfrac{2}{\beta\delta} - \delta^2$ and

$$g'(\delta) = 4\delta(\log\frac{2}{\beta\delta} - 1)$$

Accordingly, to compensate the *Cp* difference between a target and a current states, the nose angle should be changed by the following $\Delta\delta$.

$$\Delta\delta = \Delta Cp / g'(\delta) \tag{15}$$

2.5 Inverse Problem for General Slender Bodies of Revolution

The Inverse problem in this article determines geometry correction to update a baseline shape so that the updated shape realizes a target *Cp* distribution on its surface. Therefore, a design using the inverse problem here starts with a baseline shape and its surface *Cp* distribution. The idea is as follows to design the shape of general slender bodies.

The meridian plane shape of a general slender body is divided into *N* intervals and its contour curve is expressed by the connection of *N+1* grid points. The nose leading edge is located at (0, 0) and its grid coordinate is identified as ($\boldsymbol{x_0}$, $\boldsymbol{R_0}$). The coordinates of the " *i* " th grid point is ($\boldsymbol{x_i}$, $\boldsymbol{R_i}$) as shown in Fig. 4. Then, we regard the meridian plane shape as the integration of triangles each of which is constructed by the grid points of ($\boldsymbol{x_{i-1}}$, $\boldsymbol{R_{i-1}}$), ($\boldsymbol{x_i}$, $\boldsymbol{R_i}$) and ($\boldsymbol{x_i}$, $\boldsymbol{R_{i-1}}$) where $i = 1, N+1$. It is called "triangle *i*" and the angle at ($\boldsymbol{x_{i-1}}$, $\boldsymbol{R_{i-1}}$) is δ_i. We assume that Eq.(15) should hold for the ΔCp_i relation to $\Delta\delta_i$ on the piecewise "triangle *i*" because the triangle could be a meridian plane of a cone. ΔCp_i is the difference in surface Cp values between the target and current ones, calculated as

$$\Delta Cp_i = Cp_i\,(\text{target}) - Cp_i\,(\text{current}) \tag{16}$$

Cp_i is the surface *Cp* at the midpoint of the edge line, ($\boldsymbol{x_{i-1}}$, $\boldsymbol{R_{i-1}}$) and ($\boldsymbol{x_i}$, $\boldsymbol{R_i}$), *i.e.* $Cp(\boldsymbol{x_{i-1/2}})$.

Once ΔCp_i is obtained, the shape R_i^{new} to realize the target Cp_i is designed by using following equations for $i = 1, N+1$. Graphs in Fig. 4 show the updating process.

$$\Delta\delta_i = \Delta Cp_i / g'(\delta_i) \tag{17}$$

$$\delta_i^{new} = \delta_i + \Delta\delta_i \tag{18}$$

$$R_i^{new} = R_{i-1}^{new} + \delta_i^{new}(x_i - x_{i-1}) \tag{19}$$

$$\Delta R_i = R_i^{new} - R_i \tag{20}$$

3 Design System using the Inverse Problem

In this section, a design system is built using the inverse problem formulated in 2.4-2.5. The system is for general fuselage geometries including axisymmetric and quasi-axisymmetric bodies. Figure 5 illustrates the iterative process of the method. We start with an arbitrary baseline slender body shape and target *Cp* distributions. The shape is discretized in the radial (θ) direction into j_{max} intervals. For each θ station, one meridian plane exists, then totally there are j_{max}+1 planes. As one can see, when a axisysmmetric body is to be designed, j_{max} is 0.

After CFD flow analysis about the baseline shape, ΔCp is calculated. At every meridian plane, the inverse problem of Eq. (1) is solved to obtain the geometry change (Δf) to compensate the *Cp* difference. After updating all the geometry of meridian planes, we obtain a modified shape of the slender body. Using this new shape, the CFD analysis and the inverse problem process is sequentially iterated until the surface *Cp* distributions of the new shape agree with the target ones.

For the flow analysis of the method, a linearlized potential flow code [4] is used at the present. Thus the total time for one design problem is about two hours with an ordinary personal computer. When one prefers high fidelity in analysis and simulation instead of quick turn-around of design, one can conduct Navier-Stokes (N-S) flow simulation. Even if we do N-S simulation, the cost and time is not so heavy comparing with common optimization. Actually, the number of flow analysis simulation required to converge the present design process is merely up to thirty for usual design cases. Therefore, the simple and low-cost design for fuselages can be realized.

4 Design for the Nose of an Axisymmetric Fuselage

To examine the ability of the design system, an axisymmetric design has been firstly conducted. The target Cp distributions are those of a known shape which is the nose of the Sears-Haak body. A baseline (initial) geometry is one of trial products of a SST nose examined in JAXA. It is called " FC " which indicates a flared cone [5,6]. It is three-dimensionally displayed in Fig. 6. The Mach number is 1.6 and the speed of uniform flows (U) is normalized to 1. The fuselage has no angles of attack. The scaled nose length is 0.5.

Figure 7 shows the meridian plane contour of the baseline (initial) and target nose shapes as well as their *Cp* distributions along the x-axis coordinates, the plane contour curves are identical to radius distributions along the x-axis, $R(x)$. The max difference in *Cp*s is 0.0896 in the vicinity of the leading edge while that in $R(x)$ is 0.0105 at the rear.

For design process, x-axis of the body is divided into 800 non-uniform intervals. The leading edge has finer grid distribution than the other parts. After the first iteration of the proposed design system, we obtain results shown as "current R" and "Current Cp" in Fig. 8. Though the first iteration of design gives almost converged solutions, we continue the design iterations until the fifth. Finally we obtain the shape which realizes the identical *Cp* distributions to the target as shown in Fig. 9. The designed shape also agrees to the target. The errors between *Cp*s and $R(x_i)$ at each iteration step are listed in Tables 1 and 2. It takes only twenty minutes for a student to finish designing this example using a corei7 PC.

Table 1

#	Ave ERR Cp	Max ERR Cp
0	1.52.E-02	8.96.E-02
1	2.65.E-03	5.65.E-03
2	6.78.E-04	2.91.E-03
3	2.97.E-04	1.40.E-03
4	1.58.E-04	6.70.E-04
5	9.00.E-05	3.50.E-04

Table 2

#	Ave ERR in R	Max ERR in R
0	2.33.E-03	1.05.E-02
1	3.68.E-04	1.75.E-03
2	2.51.E-04	7.08.E-04
3	2.86.E-05	2.15.E-04
4	2.72.E-05	3.31.E-04
5	1.41.E-05	1.26.E-04

It should be concluded that the design system using the inverse problem formulated here is promising as a quick and precise design tool for SST noses and fuselages.

5 Design for the Laminar Nose of a SST Fuselage

The laminar SST nose has been designed using the inverse design system. This design handles a non-axisymmetric body as well as a body which has the angle of attack of 2 degrees. The body length is scaled to 0.33 by the length of a whole fuselage. It is rather a realistic design problem. The free stream Mach number was 2.0. The baseline nose shape was a cone. The shape was discretized into 36 intervals in the radial direction ($0 \le \theta \le \pi$) and 800 intervals in the x-axis direction. We have 37 meridian planes to design, thus we specify 37 target *Cp*s for each plane. Figure 10 shows the three of specified target *Cp*s, which are for the plane of θ=0, $\pi/2$ and π. The Cp distributions were devised by the SST R&D team of JAXA to attain large laminar flow region on a SST nose [7]. The initial *Cp* distributions are also there. They are the ones on the top line which means the contour line of the meridian plane of θ=0. Because the baseline shape is a cone, the initial Cps are constant on a straight line.

After 14 times of inverse design iteration, the design looks to almost reach a convergence state. The design results after the 10th iteration are exposed in Figs. 11-13. Figure 11 shows the resulting Cps and geometry as well as the target ones for the meridian plane at θ=0. So do Figs. 12 and 13 for the planes at $\theta = \pi/2$ and π, respectively. The results indicate the inverse design system proposed here is promising for the design of quasi axisymmetric body, too. However, small amount of discrepancy remains in the vicinity of the leading edge on every plane. The maximum error is on the top line. We think that the discrepancy could be settled by using Euler or Navier-Stokes calculation instead of the linearlized potential code in the design system.

The longitudinal section shape of the designed nose is shown in Fig. 14 as well as the cross section shape at x= 0.18 is in Fig. 15. In both figures axially symmetric Sears-Haack body shape is plotted to check the asymmetry of the designed shape.

6 Conclusions

Aiming to computationally design the shape of SST fuselages of good aerodynamic performance, an efficient design system has been developed. For the system the inverse problem based on the axisymmetric slender body theory has been newly formulated. The concept of the design system is iterative residual correction methodology which utilize the inverse problem to let it possible to design non-axisymmetric fuselages. The design system works well on SST nose design problems. The turn-around time to complete a design is short. It has been shown the system can handle axi-symmetric nose as well as non-axisymmetric one.

Acknowledgements

The authors thank Dr. K. Yoshida of JAXA for his honest advice. They also appreciate Mr. A. Tomita, a former trainee of JAXA and graduate of Gakushuin University, for his support in conducting inverse design on computers.

References

[1] H. Ishikawa, K. Ohira, Y. Inoue, et al. Development supersonic natural laminar flow wing design using CFD-based inverse method. *Proc. 28th ICAS congress*, Brisbane Australia, ICAS 2012- 2.2.1, Sep. 2012.

[2] Y. Ueda, K. Yoshida, K. Matsushima, H. Ishikawa. Supersonic natural-laminar-flow wing-design concept at high-Reynolds-number conditions. *AIAA Journal,* Vol. 52, No. 6, pp. 1294-1306, June 2014.

[3] H. W. Liepmann, A. Roshko. *Elements of g asdynamics*. John willey & sons, Inc., 1957. (Chapter 9)

[4] Private Communication with Dr. Kenji Yoshida, The head of SST R&D group in JAXA.

[5] T, Kawai, N. Tokugawa et al. Laminar-turbulent transition of nose boundary layer on supersonic transportation. *Proc. Annual meeting of Japan society of fluid mechanics,* p.166-169, July 2009. (in Japanese)

[6] N. Tokugawa, J. Akatsuka et. al. Surface pressure weasurement on axisymmetric bodies in Supersonic Flow. *JAXA-RM-11-016*, JAXA, ISSN 1349-1121, March. 2012.

[7] N. Tokugawa, T. Kawai et. al. Design of natural laminar flow nose for supersonic transport by wavy deformation. *JAXA-RR-13-008*, JAXA, ISSN 1349-1113, Dec. 2013.

Copyright Statement

The Contact Author Email Address is

kisam@eng.u-toyama.ac.jp

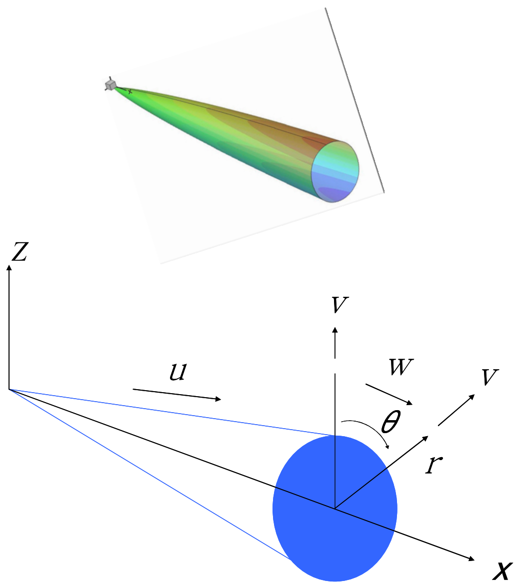

Fig. 1
Body of revolution and cylindrical coordinates.

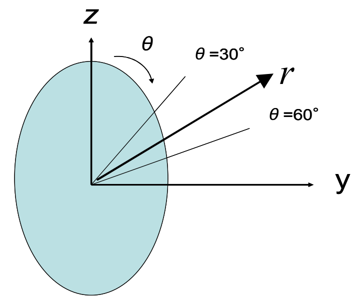

Fig.2 Cross-sectional plane.

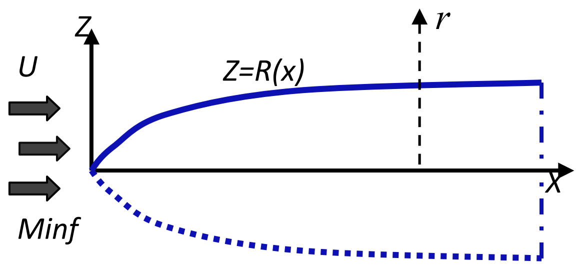

Fig.3 Longitudinal (meridian) section。

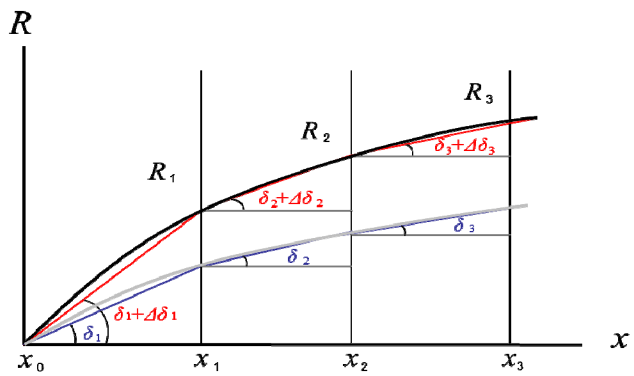

Fig. 4 Piecewise linear approximation of the current (thin lines) and updated (thick lines) shape of a meridian geometry R(x).

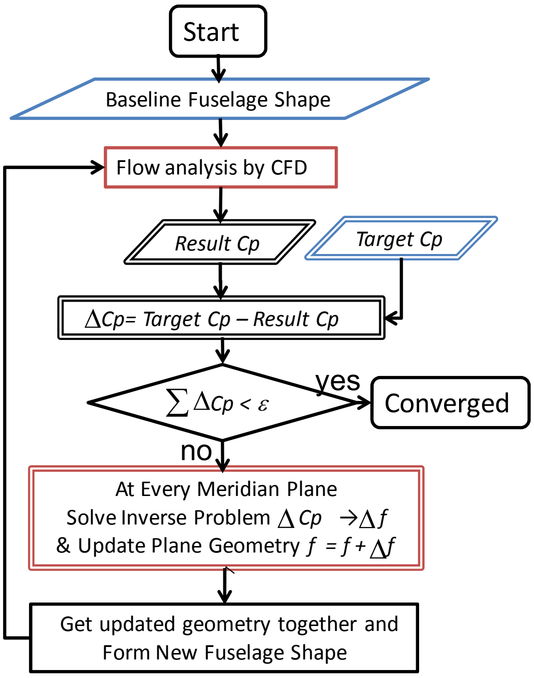

Fig. 5 Design system of iterative residual correction method using the inverse problem.

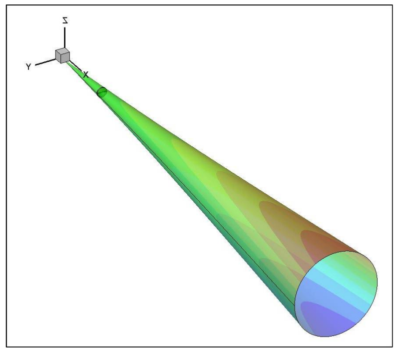

Fig. 6 The " FC " nose shape in the 3D space.

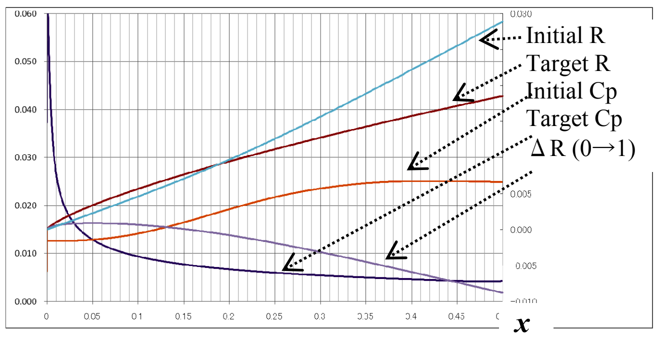

Fig. 7 Initial and target radius R and Cp distributions.

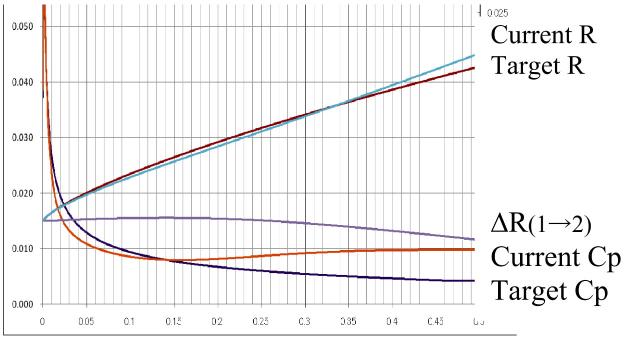

Fig. 8 Current and target radius *R* and *Cp* distributions after 1st iteration.

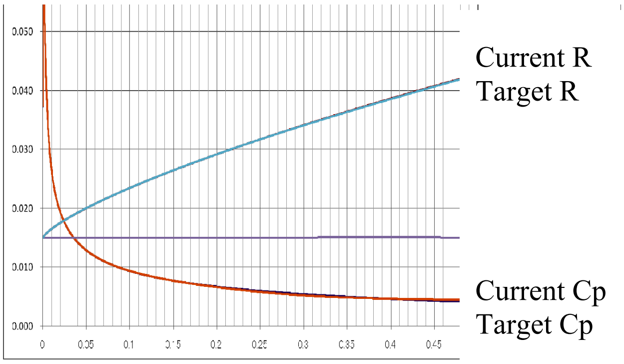

Fig. 9 Converged radius *R* and *Cp* distributions after 5th iteration.

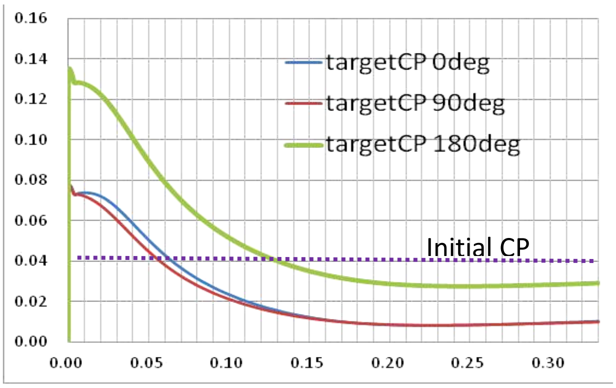

Fig. 10 Target Cps for quasi axi-symmetric shape design with initial Cps of a cone.

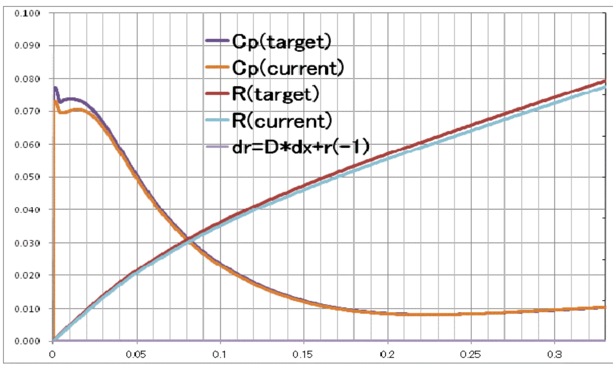

Fig. 11 Inverse design results for quasi axi-symmetric shape at θ=0.

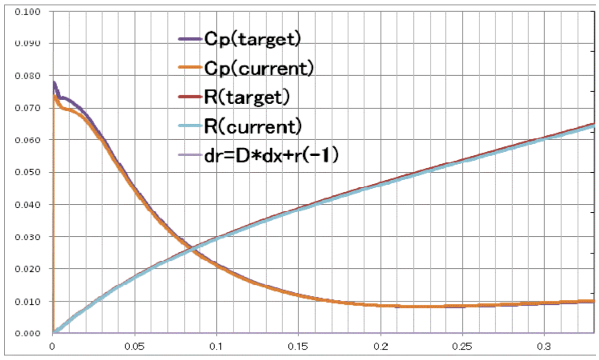

Fig.12 Inverse design results for quasi axi-symmetric shape at θ=π/2

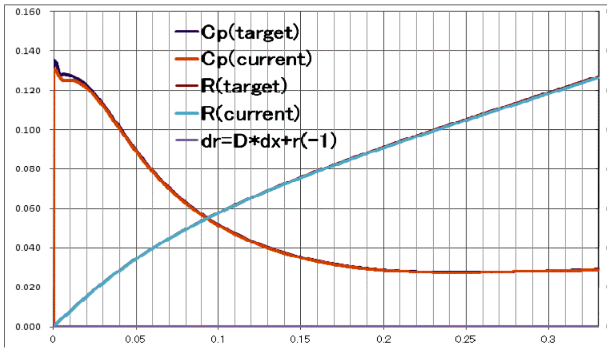

Fig. 13 Inverse design results for quasi axi-symmetric shape at θ=π.

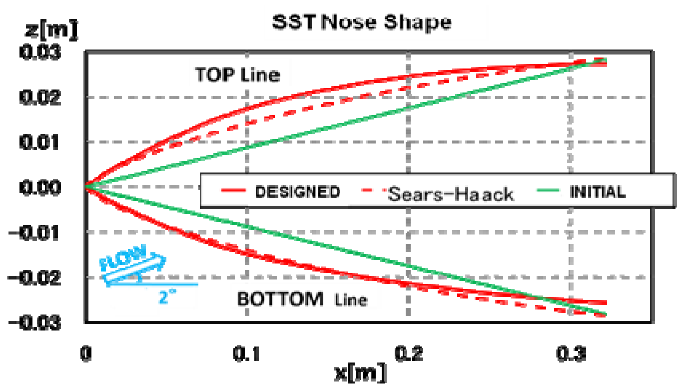

Fig. 14 Longitudinal plane of a designed nose compared with Sears-Haak and cone shapes.

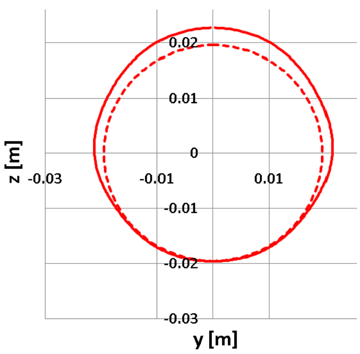

Fig. 15 Cross section shape of a designed nose compared with Sears-Haak at ***x***=0.18 of 0.33.